Eur. Phys. J. Plus (2022) 137:894
https://doi.org/10.1140/epjp/s13360-022-03115-6

THE EUROPEAN PHYSICAL JOURNAL PLUS

Regular Article

Free convection nanofluid flow past a vertical isothermal cone surface in the presence of viscous dissipation and MHD with heat flux

E. Ragulkumar[1,a], **P. Sambath**[1,b], **Ali J. Chamkha**[2,c]

[1] Department of Mathematics, SRM Institute of Science and Technology, Kattankulathur, Chennai, Tamil Nadu 603203, India
[2] Faculty of Engineering, Kuwait College of Science and Technology, Doha District 35004, Kuwait

Received: 9 February 2022 / Accepted: 26 July 2022

Abstract This study employs a numerical solution approach to examine the impacts of viscous dissipative, MHD, among various nanofluid flows across an up straight cone with iso-thermal surface velocity and temperature. After being converted into dimensionless form, the flow field equation is numerically evaluated using an outstanding finite difference approach. Our experiment used different types of nanofluids (Cu, Al_2O_3, TiO_2 and Ag) and volume fractions (0, 0.01, 0.02, 0.03, 0.04) to detect differences in heat transfer occurrence depending on temperature and velocity. Graphs have been used to show a parametric analysis for various flow field features.

List of symbols

B_0	Magnetic field induction (W m^{-2})
C_p	Specific heat at constant pressure (J kg^{-1} K^{-1})
Gr_L	Thermal Grashof number (−)
g	Acceleration due to gravity (m s^{-2})
k	Thermal conductivity (W K^{-1} m^{-1})
L	Reference length (m)
Nu_X	Non-dimensional local Nusselt number
$\overline{Nu}$	Non-dimensional average Nusselt number
Pr	Prandtl number (−)
R	Dimensionless local radius
T′	Temperature (k)
T	Dimensionless temperature
t′	Time (s)
t	Dimensionless time
U, V	Dimensionless velocity in X, Y direction
u,v	Dimensional velocity in the direction of x, y axes (ms^{-1})
x	Spatial co-ordinate alongside the cone generator (dimensional) (m)
y	Spatial co-ordinate perpendicular to cone generator (dimensional) (m)
X	Spatial co-ordinate alongside the cone generator (non-dimensional)
Y	Spatial co-ordinate perpendicular to cone generator (non-dimensional)

Greek symbols

β	Volumetric thermal expansion coefficient with temperature (K^{-1})
ϵ	Viscous dissipation parameter (−)
ϕ	Nanoparticles volume fraction (−)
μ	Dynamic viscosity (kg m^{-1} s^{-1})
μ_{nf}	Nanofluid of the dynamic viscosity (kg m^{-1} s^{-1})

[a] e-mail: ragulkumarrpv@gmail.com
[b] e-mail: sampathp@srmist.edu.in (corresponding author)
[c] e-mail: achamkha@yahoo.com

Published online: 05 August 2022

ν Kinematic viscosity (m^{-1} s^{-1})
ν_f Base fluid of the kinematic viscosity (m^{-1} s^{-1})
ω Cone apex half-angle (degree)
ρ Density (kg m^{-3})
τ_X Dimensionless local skin friction
$\overline{\tau}$ Dimensionless average skin friction

Subscripts

f Base fluid condition
nf Nanofluid condition
s Nanoparticle condition
w Wall condition
∞ Ambient condition

1 Introduction

Studying natural convection flow is essential to solve engineering and industrial problems. Such flows are controlled by the density difference and the flow affects heat transmission. It is commonly used to study the magnetic field and velocity in electrically conducting fluids such as liquid metals, plasmas as well as astrophysical phenomena. As a result of their increased thermal conductivity, nanofluids have a wide range of applications in a variety of industries. Additionally, nanofluids can be used as brake and engine lubricants as well as radiator coolants in automobiles. Nanofluids are extraordinary fluids with a higher thermal conductivity. The concept of uniform surface heat flux was initially proposed in the literature by Lin [1]; he determined the flow of laminar plain convective from a upright circular cone with constant wall flux. Na and Chiou [2] resolved the differential equations that govern the solutions of natural convection flow past a thin frustum in a cone with a constant heat flux through the wall. Pop and Watanabe [3] studied steady plain convective current from a up straight cone with uniform surface heat flux focusing on the effects of suction or injection. Choi et al. explored [4] physical considerations for explaining the anomalous thermal characteristics of nanotube suspensions. Hossain and Paul [5] were examined relevant parameters to determine how laminar plain convective peripheral layers current from a plumb cone with uneven surface heat flux.

The stratified parameters affect laminar plain convective current from a up straight circular cone with a even surface temperature and a constant surface heat flux, as addressed by Hossain et al. [6]. A numerical study has been investigated by Ganesan and Palani [7] for the MHD flow past a semi-infinite slanted plate with variable surface heat and mass flux. Kumari and Nath [8] conducted a more general investigation of non-Darcy flow across a upright cone immersed in a saturated porous media. A 2D unstable laminar incompressible peripheral layer model has been implemented by Mohiddin et al. [9] to handle both external flow and heat transfer in viscoelastic buoyancy-driven convection regimes past a up straight stationary cone. CY Cheng [10] studied the impact of Soret as well as Dufour on the peripheral layer flow caused by plain convective heat as well as mass transfer around a plumb cone in a fluid-saturated porosity media with continuous wall heat as well as mass fluxes.

The heat transfer properties of naturally convective via a vertical cone when a magnetic field and thermal radiation are present were studied by Palani and Kim [11]. A transverse magnetic field interferes with the free convection flow over an upright cone with a varying surface external heat flux, as described by Palani et al. [12]. The effect of homogeneous mass flux on non-Darcy convection was investigated by Chamkha et al. [13] with upright cone embedded in a highly permeable medium containing nanofluid. Among other topics, Narahari et al. [14] discussed 2D convection of a multiphase nanofluid past a vertical plate with constant thermal flux in two dimensions. Sambath et al. [15] derived the governing equation for a vertical cone with natural convective MHD in the presence of a radiated chemical reaction by using the Crank-Nicolson method. The characteristics of the flow of incompressible viscous fluid via an upright cone under inhomogeneous mass flux were studied by Sambath et al. [16].

Here, our objective is to investigate free convection nanofluid flow across a vertical isothermal cone surface with viscous dissipation and MHD with heat flux unless someone else has already done so. The heated vertical cone substance is submerged in a fluid containing nanoparticles. The heat transfer from that cone takes place in the fluid here; we examine how the heat transfer occurs in the nanofluid rather than the fluid.

The remainder of this paper is structured as follows; in Sect. 2, mathematical modeling of the problem is given along with physical model, governing equation and boundary conditions. In Sect. 3, the method of solution to solve the governing equation with the help of boundary conditions is discussed. In Sect. 4, the outcomes of findings are listed and discussed graphically. Finally in Sect. 5, we made some concluding remarks of the problem analyzed.

2 Mathematical modeling

The heat flux represents a 2-dimensional unstable boundary layer flow across an isothermal permeable cone surface with MHD using a distinct nanofluid. The mathematical model of the problem as well as the flow configuration and coordinate system is displayed in Fig. 1. T'_∞ denotes the temperature difference between the cone's surface and the surrounding liquid at a given temperature. Once this temperature $T'_W(x)$ is reached, the surface of the cone is maintained at that level until time $t' > 0$. Marneni Narahari [14] shows four types of nanoparticles (Cu, Al_2O_3, TiO_2 and Ag) and their thermal characteristics in Table 1. These nanoparticles are spherical in form. The fluid's properties are believed to be constant with the exception of density variations. Under the influence of the Boussinesq approximation, the basic equations that regulate the flow, continuity, momentum and energy are listed below:

Equation of Continuity

$$\frac{\partial(ru)}{\partial x} + \frac{\partial(rv)}{\partial y} = 0 \tag{1}$$

Equation of Momentum

$$\frac{\partial u}{\partial t'} + u\frac{\partial u}{\partial x} + v\frac{\partial u}{\partial y} = g\frac{(\rho\beta_T)_{nf}}{\rho_{nf}}(T' - T'_\infty)\cos\omega + v_{nf}\frac{\partial^2 u}{\partial y^2} - \frac{\sigma B_0^2}{\rho_{nf}}u \tag{2}$$

Equation of Energy

$$\frac{\partial T'}{\partial t'} + u\frac{\partial T'}{\partial x} + v\frac{\partial T'}{\partial y} = \frac{k_{nf}}{(\varrho c_p)_{nf}}\frac{\partial^2 T'}{\partial y^2} + \frac{\mu_{nf}}{(\varrho c_p)_{nf}}\left(\frac{\partial u}{\partial y}\right)^2 \tag{3}$$

Initial and boundary condition are

$$t' \le 0 : u = 0, v = 0, T' = T'_\infty \quad \text{for all x and y}$$
$$t' > 0 : u = 0, v = 0, \quad \frac{\partial T'}{\partial y} = \frac{-q_w x}{k} \quad \text{at y=0}$$
$$u = 0, v = 0, \quad T' = T'_\infty \quad \text{at x=0}$$

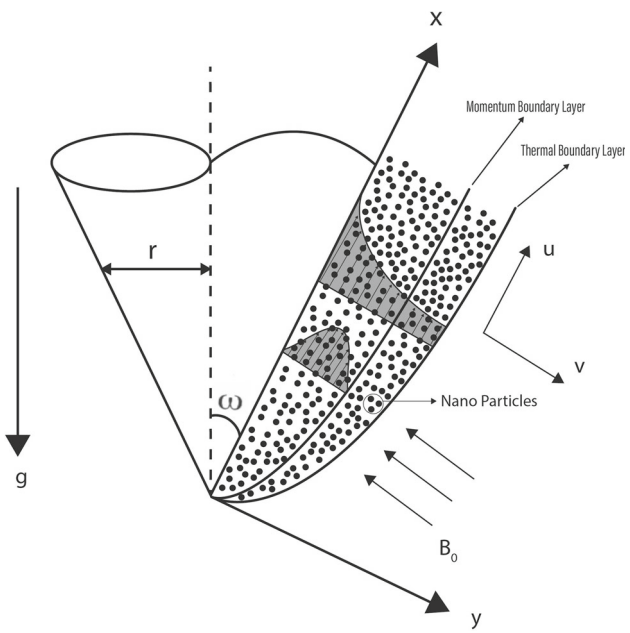

Fig. 1 Physical model and coordinate system

Table 1 Thermo-physical properties of water and nanoparticles

Physical features	Water	Copper	Silver	Aluminum oxide	Titanium dioxide
$\bar{\rho}$ (kg m^3)	997.10	8933.0	10500	3970.0	4250.0
$\bar{C}_{\bar{p}}$ (J/kgK)	4179.0	385.0	235	765.0	686.2
$\bar{k}$ (W/mK)	0.613	401.0	429	40.0	8.9538
$\bar{\beta} \times 10^{-5}$ (K^{-1})	21.0	1.67	1.89	0.85	0.90

$$u = 0, v = 0, \ T' \to T'_\infty \quad \text{as } y \to \infty \tag{4}$$

For nanofluids, the expressions of density ρ_{nf}, thermal expansion co-efficient $(\rho\beta)_{nf}$ and heat capacitance $(\rho c_p)_{nf}$ are given by

$$\begin{aligned}
&\rho_{nf} = (1-\phi)\rho_f + \phi\rho_s \\
&(\rho\beta)_{nf} = (1-\phi)(\rho\beta)_{nf} = (1-\phi)(\rho\beta)_f + \phi(\rho\beta)_s \\
&(\rho c_p)_{nf} = (1-\phi)(\rho c_p)_{nf} = (1-\phi)(\rho c_p)_f + \phi(\rho c_p)_s \\
&\frac{k_{nf}}{k_f} = \frac{k_s + (n-1)k_f - (n-1)\phi(k_f - k_s)}{k_s + (n-1)k_f + \phi(k_f - k_s)} \\
&\frac{\mu_{nf}}{\mu_f} = \frac{1}{(1-\phi)^{2.5}}
\end{aligned}$$

Dimensionless quantities are

$$\begin{aligned}
X = \frac{x}{L}, \ Y = \frac{y}{L}Gr_L^{1/5}, \ U = \frac{uL}{\nu_f}Gr_L^{-2/5}, \ V = \frac{vL}{\nu_f}Gr_L^{-2/5} \\
t = \frac{\nu_f t'(Gr_L)^{2/5}}{L^2}, \ T = \frac{T' - T'_\infty}{(q_w(L)L/k)}Gr_L^{1/5}, \ Gr_L = \frac{g\beta q_w(L)L^4 cos\omega}{k\nu_f^2}, \\
Pr = \frac{\nu_f}{\alpha_f}, M = \frac{\sigma B_0^2 L^2}{\mu_{nf}}Gr_L^{-2/5}, \ R = \frac{r}{L}; \ \ r = x\ sin\ \omega;
\end{aligned} \tag{5}$$

Equation of Continuity

$$\frac{\partial U}{\partial X} + \frac{\partial V}{\partial Y} + \frac{U}{X} = 0 \tag{6}$$

Equation of Momentum

$$\frac{\partial U}{\partial t} + U\frac{\partial U}{\partial X} + V\frac{\partial U}{\partial Y} = (A_1)\Big[(T) - MU\Big] + (A_2)\frac{\partial^2 U}{\partial Y^2} \tag{7}$$

Equation of Energy

$$\frac{\partial T}{\partial t} + U\frac{\partial T}{\partial X} + V\frac{\partial T}{\partial Y} = \frac{k_{nf}}{k_f}\frac{1}{Pr}(A_3)\frac{\partial^2 T}{\partial Y^2} + (A_4)\,\epsilon\left(\frac{\partial U}{\partial Y}\right)^2 \tag{8}$$

where

$$\begin{aligned}
A_1 = \frac{(1-\phi) + \phi\frac{(\rho\beta)_s}{(\rho\beta)_f}}{(1-\phi) + \phi\frac{\rho_s}{\rho_f}}, A_2 = \frac{1}{(1-\phi)^{2.5}\left(1 - \phi + \phi\frac{\rho_s}{\rho_f}\right)} \\
A_3 = \frac{1}{(1-\phi) + \phi\frac{(\rho c_p)_s}{(\rho c_p)_f}}, A_4 = \frac{1}{(1-\phi)^{2.5}\left(1 - \phi + \phi\frac{(\rho c_p)_s}{(\rho c_p)_f}\right)}
\end{aligned}$$

Non-dimensional initial and boundary condition are

$$\begin{aligned}
&t' \le 0: \ U = 0, V = 0, T = 0 \quad \text{for all X and Y} \\
&t' > 0: \ U = 0, V = 0, \ \frac{\partial T}{\partial Y} = -1 \quad \text{at Y = 0} \\
&U = 0, \ T = 0 \quad \text{at X = 0} \\
&U \to 0 \ T \to 0 \quad \text{as Y} \to \infty
\end{aligned} \tag{9}$$

The non-dimensional local skin friction [11] and the local Nusselt number [16] are calculated as follows:

$$\tau_X = \frac{1}{(1-\phi)^{2.5}}Gr^{3/5}\left(\frac{\partial U}{\partial Y}\right)_{Y=0} \tag{10}$$

$$Nu_X = \frac{k_{nf}}{k_f}\frac{-X\left(\frac{\partial T}{\partial Y}\right)_{Y=0}Gr^{1/5}}{T_{Y=0}} \tag{11}$$

In addition, the non-dimensional average skin friction and the average Nusselt number are provided by:

$$\bar{\tau} = \frac{2}{(1-\phi)^{2.5}} Gr^{3/5} \int_0^1 X \left(\frac{\partial U}{\partial Y}\right)_{Y=0} dX \tag{12}$$

$$\overline{Nu} = 2\frac{k_{nf}}{k_f} Gr^{1/5} \int_0^1 \frac{-X\left(\frac{\partial T}{\partial Y}\right)_{Y=0}}{T_{Y=0}} dX \tag{13}$$

3 Solution methodology

The system of nonlinear PDE's in Eqs. (6)–(8) under boundary condition (9) is computationally solved by employing the Thomas algorithm and indeed the Crank-Nicolson technique via the finite difference method. A grid representing the integral region is visualized as a square with the boundary X_{max} (= 1.0) as well as Y_{max} = (20) for calculation purposes. Hence, Y_{max} usually refers to $Y = \infty$, which is far enough away from the velocity and thermal peripheral layers. After that, the highest value of Y which satisfied remaining two boundary conditions (9) was determined by exploratory research. According to our analysis, the tolerance limit of 10^{-5} has been correctly achieved.

The calculation was carried out by lowering the spatial grid sizes by 50% in one direction and then by 50% on both sides. The suggested method is both consistent and completely stable, indicating that the scheme is convergent. According to [14] the calculations are carried out for four types of nanoparticles employing water as the base fluid for varied values of the nanoparticle volume fraction. These results are based on silver (Ag), copper (Cu), aluminum oxide (Al_2O_3) and titanium oxide (TiO_2) nanofluids as well as volume fraction of nanoparticles (ϕ) varied from 0 to 0.04.

4 Results and findings

The major purpose of this study is to obtain a detailed understanding of a fluid model; the effects of various parameter values on U, T contours are numerically computed and diagrammatically depicted. Figures 2, 3, 4, 5, 6, 7, 8, 9, 10, 11, 12, 13, 14, 15, 16, 17 as well as Table 1 along with different regulatory parameters Pr, M, ε and ϕ are used in our mathematical simulation unless otherwise indicated. We observed variability in velocity, temperature distribution, skin friction coefficient as well as heat transfer rate under the influence of various nanofluids. In the case of a particular parameter being modified, all other parameters are taken to remain constant.

4.1 Temperature and velocity

The numerical values of MHD and viscous dispersion in terms of velocity and temperature, for the distinct nanofluids and volume fractions, are illustrated in Figs. 2, 3, 4, 5, 6, 7, 8, 9. As shown in Figs. 2 and 3 aluminum oxide (Al_2O_3) nanoparticles enhance free convective heat transfer better than other nanofluids because their reduction potential will tend to lose electrons to the new species. Figures 4 and 5 demonstrate the effect of ϕ on the temperature and velocity curve when Pr = 6.2, M = 1 and ε = 0.6. In these diagrams, the streamline can be seen for various ϕ values and it can be noticed that as nanoparticle of volume fractions increases from 0 to 0.04 for different nanoparticles, the velocity and temperature decrease because of the absorbent nature of added nanoparticles.

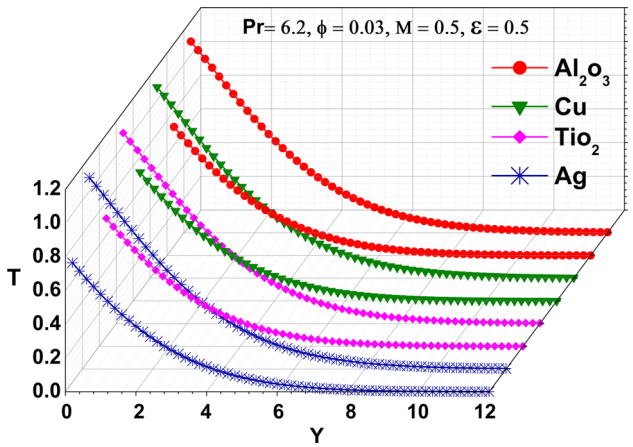

Fig. 2 The fluid temperature gradient for various nanofluids

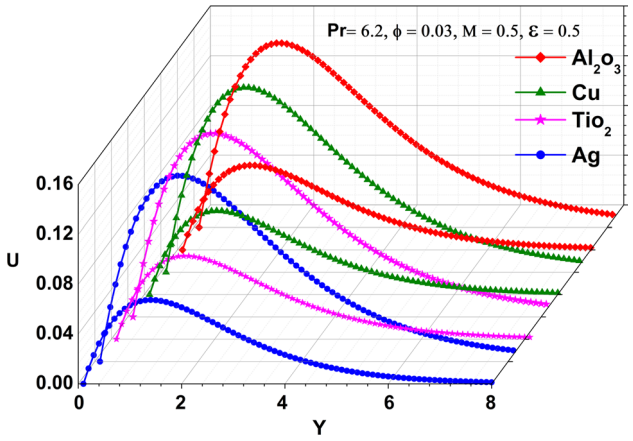

Fig. 3 The fluid velocity gradient for various nanofluids

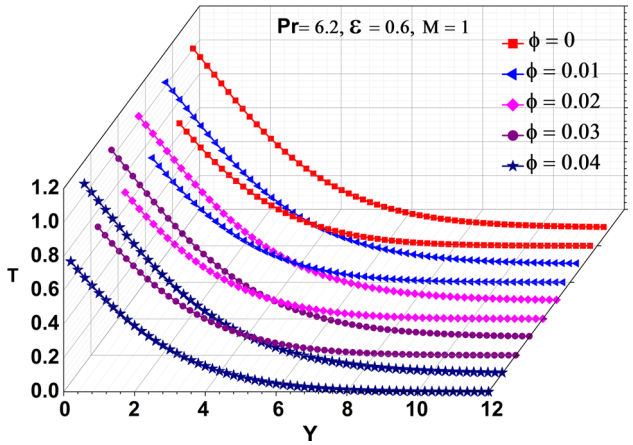

Fig. 4 The fluid temperature gradient for various volume fraction (ϕ)

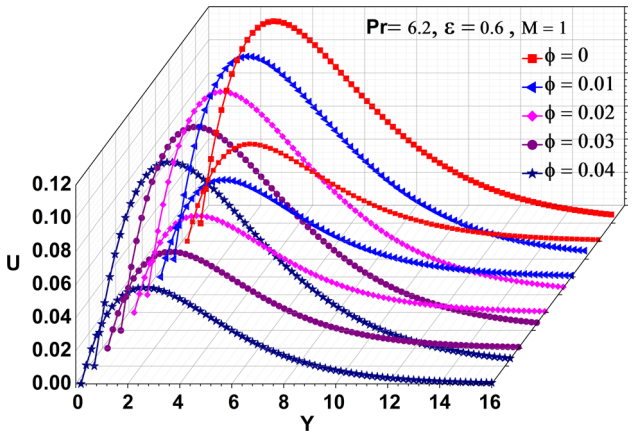

Fig. 5 The fluid velocity gradient for various volume fraction (ϕ)

Temperature and velocity profiles of different nanofluid phases are shown in Figs. 6 and 7 as a function of a magnetic parameter (M). In subsequent experiments, the thickness of the thermal and momentum boundary layers decreased when the magnetic parameter was increased. As a magnetic field is applied to water-based nanofluids, the thermal motion of partially charged atoms results in Lorentz forces, which cause the temperature and velocity to decrease.

A temperature and velocity profile using the dissipation parameter (ε) is displayed in Figs. 8 and 9. These graphs depict when increasing the viscous dissipation parameter (ε) generates a worsening in the temperature and velocity profiles as well as the thermal and momentum boundary layer thickness, due to heat transfer through shear forces caused by fluid flow in the surrounding layers.

4.2 Local and average Nusselt number as well as local and average skin friction

The effects of amplified volume fraction on local skin friction (τ_X) and local Nusselt number (Nu_X) fluctuation throughout its axial coordinate X are shown in Figs. 10 and 11. Figure 10 shows that when the nanoparticle volume fraction parameter (ϕ) is increased,

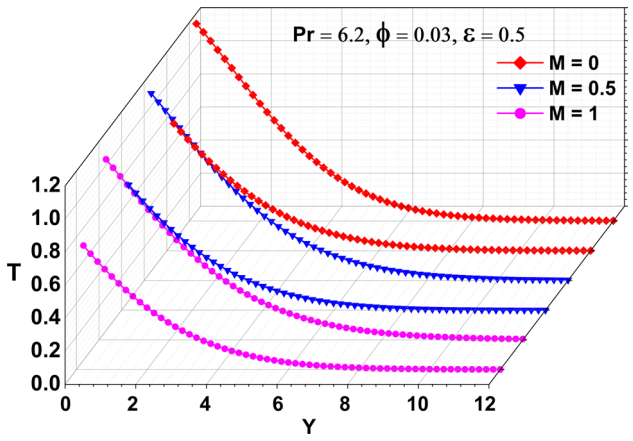

Fig. 6 The fluid temperature gradient for various M values

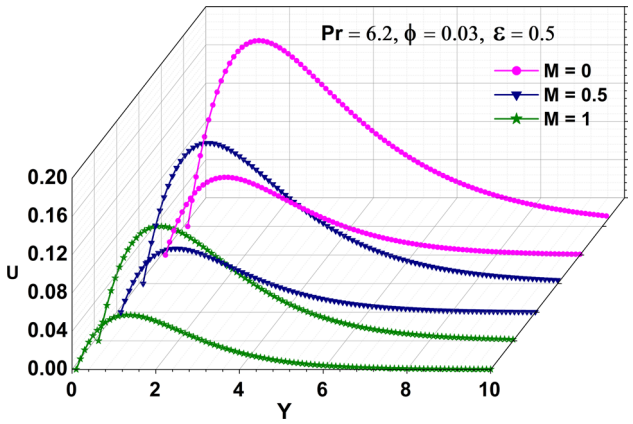

Fig. 7 The fluid velocity gradient for various M values

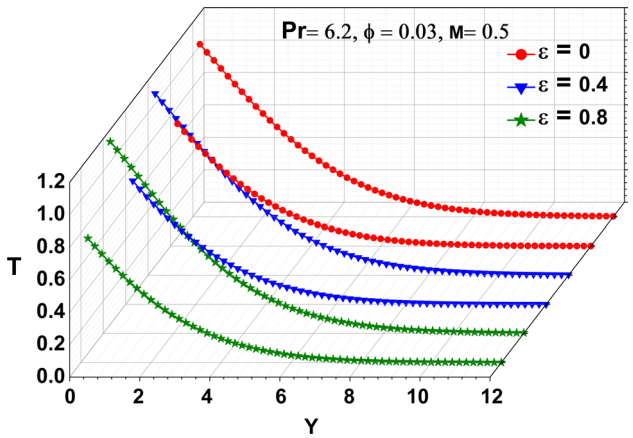

Fig. 8 The fluid temperature distribution for various ε value (viscous dissipation)

the local skin friction τ_X decreases until a steady-state value of the friction is reached. Also, once the nanoparticle volume fraction parameters (ϕ) increase, the local Nusselt number (Nu_X) decreases in water-based nanofluids along the cone surface, as illustrated in Fig. 10. The Figs. 12 and 13 illustrate the effects of local Nusselt number and skin friction on the convection coefficient of nanofluids with aluminum oxide nanomaterials proving to be far more effective at improving free convection heat transfer since the aluminum oxide is amphoteric and "oxide ions" are confined to the solid lattice and are capable of reacting with water molecules. As compared to the other nanofluids tested, aluminum oxide was found to have a higher tendency to coat the surface of the cone.

As shown in Figs. 14 and 15, the effects of increasing the volume fraction upon average skin friction ($\overline{\tau}$) as well as average Nusselt number ($\overline{Nu}$) change along the axial direction X. Using figure 14, it is easy to realize that the average skin friction decreases as the nanoparticle volume fraction parameter (ϕ) is increased although a steady-state value has been reached. In this case, we can observe what happens with the average skin friction ($\overline{\tau}$) as a function of increasing volume fraction. Moreover, according to Fig. 15, the Nusselt number of water-based nanofluids across the entire cone surface decreases with the increase of volume fraction parameters within nanoparticles (ϕ). Similarly, Figs. 16 and 17 usually portray the average Nusselt number and skin friction curves over many

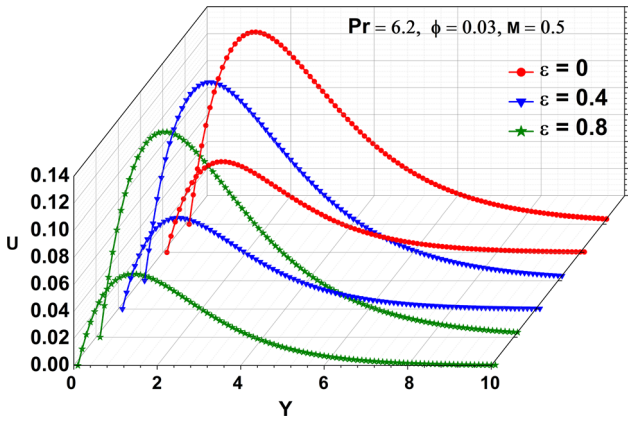

Fig. 9 The fluid velocity distribution for various ε value (viscous dissipation)

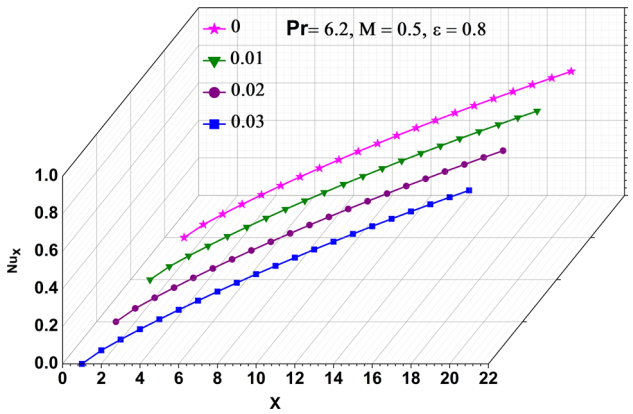

Fig. 10 Functional dependence of the local Nusselt number for various ϕ (volume fraction)

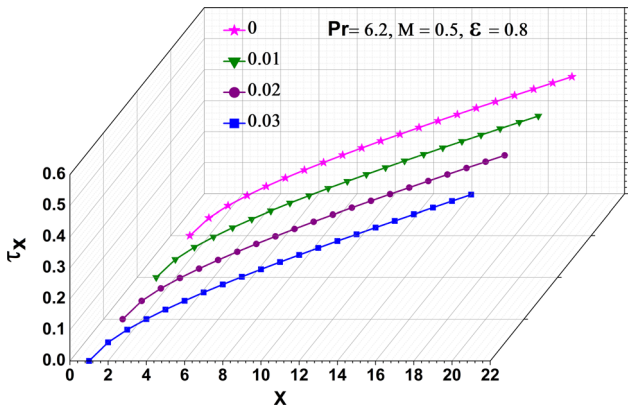

Fig. 11 Functional dependence of the local skin friction for various ϕ (volume fraction)

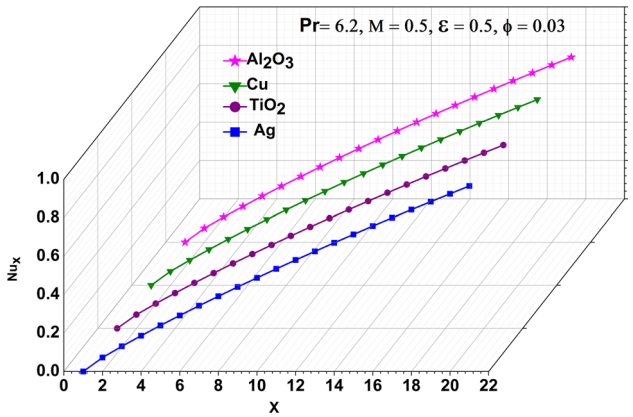

Fig. 12 Functional dependence of the local Nusselt number for various nanofluid

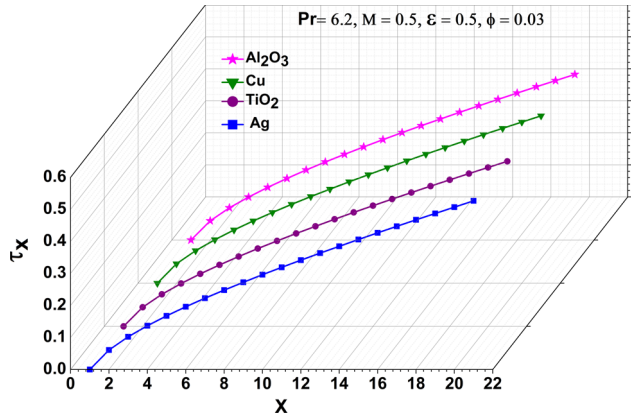

Fig. 13 Functional dependence of the local skin friction for various nanofluid

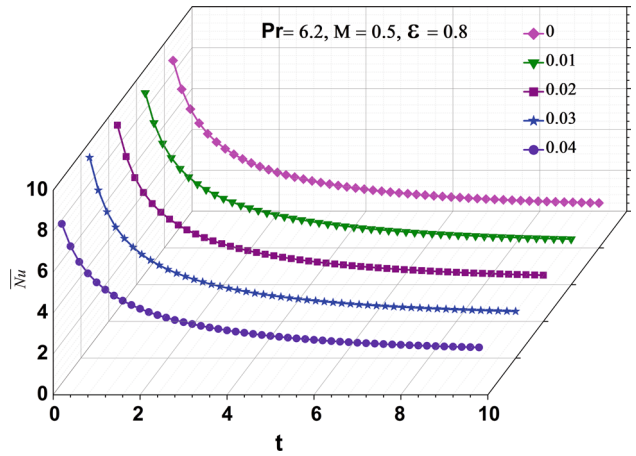

Fig. 14 Functional dependence of the average Nusselt number for various ϕ (volume fraction)

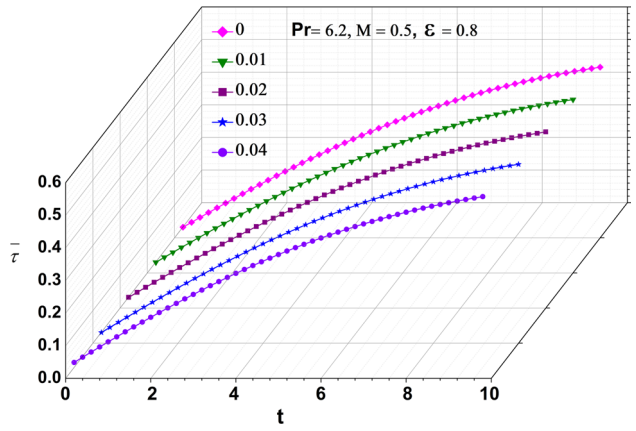

Fig. 15 Functional dependence of the average skin friction for various ϕ (volume fraction)

nanofluids, correspondingly. The researchers used a variety of nanofluids with aluminum oxide nanomaterials proving to be the most effective in enhancing free convection. It was found that aluminum oxide had a greater tendency to adhere to the surface of the cone than the other nanofluids.

The study in this section illustrates how heat transfer by free convection from a heated vertical cone using various nanofluids occurs due to the impact of viscous dispersion on the boundary layer surface and the additional effects of magnetohydrodynamics on the velocity and temperature distribution. Furthermore, the predominance of any nanofluid during heat transfer by reacting with viscous dispersion and magnetohydrodynamics as a result of the addition of nanofluidic fluids and the changes resulting in free convection at the boundary layer surface are explained in terms of skin friction coefficient and heat transfer rate.

Heat is transferred by free convection when free electrons or lattice vibrational waves are displaced in the heat conduction. Although heat transmission by conduction is dependent on the driving "force" of the temperature differential, it is different in the presence of fluid motion for convection. The energy flow is purely through conduction on the cone's surface, but in the next layers,

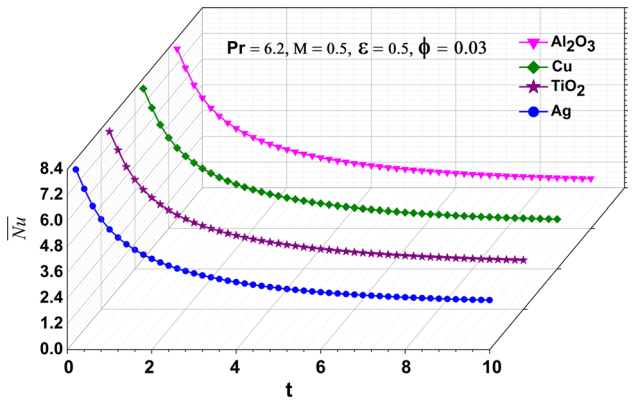

Fig. 16 Functional dependence of the average Nusselt number for various nanofluid

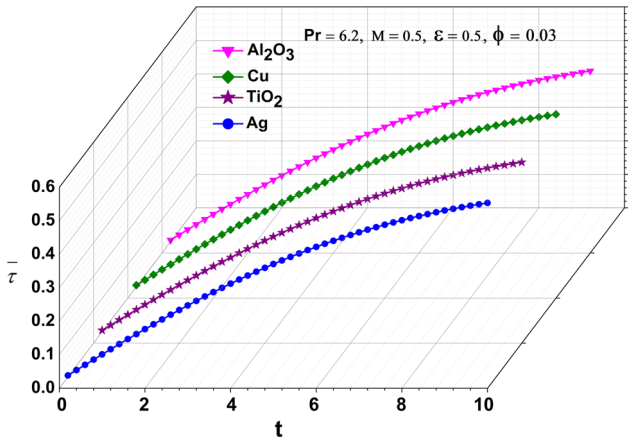

Fig. 17 Functional dependence of the average skin friction for various nanofluid

both conduction and diffusion-mass motion occurs at the molecular or macroscopic levels. The given figures show that the energy transfer rate is high due to mass movement.

5 Discussion with conclusion

The ultimate aim of this presentation is to describe the flow behavior of a distinctive nanofluid's MHD boundary layer flow through a permeable vertical cone surface, with significant effects of viscous dissipation and heat flux. A decrease in both temperature and velocity components was observed as the volume fraction of nanofluid, the dissipation parameter as well as magnetic field increased. Among the nanofluids investigated, Al_2O_3-water nanofluid has the greatest temperature and velocity components inside the computational domain, whereas Ag-water nanofluid has the lowest.

Since the volume fraction coefficient increases, both the local skin friction coefficient and the Nusselt number decrease. The largest and lowest responses to local Nusselt number and skin friction contours are seen in Al_2O_3-water and Ag-water, respectively. In addition to the average Nusselt number and the skin friction coefficient, both decrease when the volume fraction coefficient increases. The average Nusselt number within the computational domain is maximal for Al_2O_3-water nanofluid and minimum for Ag-water nanofluid. The average skin friction in Al_2O_3-water nanofluid is the highest, whereas in Ag -water nanofluid the lowest.

Author Contributions ERK, PS and AJC conceived and designed the study. ERK conducted the literature search and drafted the manuscript. PS and AJC were involved in the analysis and interpretation of data. The study was supervised by PS. All authors read and approved the final manuscript.

Data availability The datasets supporting the conclusions of this article are included within the article.

Declarations

Conflicts of interest The authors declare that they have no competing interests.

References

1. F.N. Lin, Laminar free convection from a vertical cone with uniform surface heat flux. Lett. Heat Mass Transf. **3**, 49–58 (1976)
2. T.Y. Na, J.P. Chiou, Laminar natural convection over a slender vertical frustrum of a cone with constant wall heat flux. Wärme-und Stoffübertragung **13**(1), 73–78 (1980)
3. I. Pop, T. Watanabe, Free convection with uniform suction or injection from a vertical cone for constant wall heat flux. Int. Commun. Heat Mass Transf. **19**(2), 275–283 (1992)
4. S.U.S. Choi, Z.G. Zhang, W. Lockwood, F.E. Yu, F.E. Lockwood, E.A. Grulke, Anomalous thermal conductivity enhancement in nanotube suspensions. Appl. Phys. Lett. **79**(14), 2252–2254 (2001)
5. M.A. Hossain, S.C. Paul, Free convection from a vertical permeable circular cone with non-uniform surface heat flux. Heat Mass Transf. **37**(2), 167–173 (2001)
6. M.A. Hossain, S.C. Paul, A.C. Mandal, Natural convection flow along a vertical circular cone with uniform surface temperature and surface heat flux in a thermally stratified medium. Int. J. Numer. Methods Heat Fluid Flow **2**, 5586 (2002)
7. P. Ganesan, G. Palani, Finite difference analysis of unsteady natural convection MHD flow past an inclined plate with variable surface heat and mass flux. Int. J. Heat Mass Transf. **47**(19–20), 4449–4457 (2004)
8. M. Kumari, G. Nath, Natural convection from a vertical cone in a porous medium due to the combined effects of heat and mass diffusion with non-uniform wall temperature/concentration or heat/mass flux and suction/injection. Int. J. Heat Mass Transf. **52**(13–14), 3064–3069 (2009)
9. S. Mohiddin, S. Gouse, V.K. Varma, N. Iyengar, Unsteady viscoelastic free convection boundary layerflow past a vertical cone with uniform heat and mass flux". J. Comput. Math. Sci. **1**(2), 103–273 (2010)
10. C.-Y. Cheng, Soret and Dufour effects on natural convection boundary layer flow over a vertical cone in a porous medium with constant wall heat and mass fluxes. Int. Commun. Heat Mass Transf. **38**(1), 44–48 (2011)
11. G. Palani, K.Y. Kim, Influence of magnetic field and thermal radiation by natural convection past vertical cone subjected to variable surface heat flux. Appl. Math. Mech. **33**(5), 605–620 (2012)
12. G. Palani, A.R. Ragavan, E. Thandapani, Effect of viscous dissipation on an MHD free convective flow past a semi-infinite vertical cone with a variable surface heat flux. J. Appl. Mech. Tech. Phys. **54**(6), 960–970 (2013)
13. C. Ali, S. Abbasbandy, A.M. Rashad, Non-Darcy natural convection flow for non-Newtonian nanofluid over cone saturated in porous medium with uniform heat and volume fraction fluxes. Int. J. Numer. Methods Heat Fluid Flow **2**, 558 (2015)
14. M. Narahari, Unsteady free convection flow past a semi-infinite vertical plate with constant heat flux in water based nanofluids. IOP Conf. Ser. Mater. Sci. Eng. **342**(1), 012085 (2018)
15. P. Sambath, B. Pullepu, T. Hussain, S.A. Shehzad, Radiated chemical reaction impacts on natural convective MHD mass transfer flow induced by a vertical cone. Results Phys. **8**, 304–315 (2018)
16. P. Sambath, D.S. Sankar, K.K. Viswanathan, A numerical study of dissipative chemically reactive radiative MHD flow past a vertical cone with nonuniform mass flux. Int. J. Appl. Mech. Eng. **25**(1), 5598 (2020)